6th European Conference on Computational Mechanics (ECCM 6)
7th European Conference on Computational Fluid Dynamics (ECFD 7)
11-15 June 2018, Glasgow, UK

HEMODYNAMICS IN THE PULMONARY BIFURCATION IN RELATION TO ADULTS WITH CONGENITAL HEART DISEASE: EFFECT OF BRANCHING ANGLE AND ORIGIN

MARIA BOUMPOULI[1], MARK DANTON[2], TERENCE GOURLAY[1] AND ASIMINA KAZAKIDI[1,*]

[1] Department of Biomedical Engineering, University of Strathclyde, Glasgow G4 0NW, UK
{maria.boumpouli, terence.gourlay, * asimina.kazakidi}@strath.ac.uk

[2] Scottish Adult Congenital Cardiac Service, Golden Jubilee National Hospital, Clydebank G81 4DY, UK

Key words: Computational fluid dynamics, pulmonary valve replacement, congenital heart disease, tetralogy of Fallot

Abstract. Pulmonary regurgitation is the most common, clinically-important, complication that affects an increasing population of adult patients with congenital heart disease, primarily with repaired tetralogy of Fallot. Without intervention, the condition can lead to abnormal dilatation of the right ventricle, arrhythmias, heart failure, or death. Pulmonary valve replacement (PVR) is a frequent re-operation, the clinical decision for which is currently relying on symptoms, including arrhythmias and measures of the right ventricular volume. However, there is no common consensus on the reliability of these criteria and further studies are needed for an accurate and timely assessment for PVR treatment. The overall objective of this work is to hemodynamically characterise the pulmonary bifurcation in adult patients with congenital heart disease, pre- and post-operatively, and help establish novel metrics for a more accurate assessment for PVR, contributing to better surgical planning. In this study, we present preliminary computational fluid dynamic results in simplified models of the pulmonary trunk and its branches, in order to investigate the effect of the bifurcation angle on the flow. Physiological vessel dimensions and boundary conditions were used, in both symmetric and asymmetric geometries, and blood flow was simulated by solving the incompressible Navier-Stokes equations. Increase of the branching angle altered the flow development within the bifurcation, and had evident effects on the flow separation downstream of the junction. Shear stresses on the wall connecting the two artery branches were found, for the first time, dependent also on the origin of each branch, having a greater effect on the left pulmonary artery. These results demonstrate the impact of geometry on velocity, pressure, and wall shear stresses in the pulmonary bifurcation and contribute to a better understanding of the underlying flow mechanisms. Future studies will involve 3D reconstruction of patient-specific models of the pulmonary bifurcation, obtained from MRI images of adult patients with repaired tetralogy of Fallot, that need or have undergone pulmonary valve replacement.

1 INTRODUCTION

Congenital Heart Disease (CHD) lesions occur during embryonic development and are defined, according to Mitchell et al. [1], as *'gross structural abnormalities of the heart or intrathoracic great vessels that is actually or potentially of functional significance'*. During the '50s, only 10-15% of newborns with such lesions survived until puberty [2]. However, due to advancements in medical diagnostic modalities and the success of paediatric surgical procedures, over the last decades, most children survive to adulthood and, as a result, a new cohort of patients exists that is no longer limited to paediatric clinical practice [3]. This increasing population of adult patients with CHD experience complex cardiovascular abnormalities which require specialised medical attention, including frequent monitoring, re-operations, and new surgical treatments [4].

Tetralogy of Fallot (ToF) can be considered one of the most common cyanotic types of CHD. Patients suffering from ToF are diagnosed with four defects: a ventricular septal defect, an overriding aorta, pulmonary stenosis, and right ventricular hypertrophy [5]. These are usually detected in infancy and surgical repair is recommended to prevent cyanosis. Although patients with repaired defects have long survival rates and they live unobstructed lives, they are at risk of chronic complications. Pulmonary artery kinking, which can cause stenosis of the left pulmonary artery (LPA), and pulmonary valve regurgitation, in which blood can leak back to the right ventricle, are some of the most frequent indications for surgical re-intervention [6, 7, 8]. Pulmonary regurgitation, a frequent consequence of the repair of the right ventricular outflow tract, can be tolerated for long periods, especially if the leak is mild to moderate; when severe and chronic conditions arise, however, it ultimately leads to right ventricular dilatation and dysfunction. LPA re-stenosis exacerbates right ventricular function [9], and pulmonary valve replacement (PVR) is deemed necessary in the cases of severe valve regurgitation [6, 7, 10]. Assessment of the clinical indications and the right timing for PVR is a key challenge for clinicians. The clinical decision for surgical intervention is currently relying on symptoms, including arrhythmias, and measures of right ventricular dilatation, at e.g. 80-90 mL/m^2 end-systolic and 150-160 mL/m^2 end-diastolic volumes [11, 12]. However, the reliability of these criteria is yet ambiguous and the correct timing for surgical treatment of asymptomatic regurgitation cases remains an open question [7].

Computational fluid dynamics (CFD) can be used as a tool to help the assessment of cardiovascular diseases, through quantification of hemodynamic parameters, such as velocity, pressure, and wall shear stresses. Computational models can, therefore, support clinical diagnosis, treatment, and surgical planing [13]. In that context, there is a number of previous studies that investigate the blood flow in the pulmonary arteries of congenital heart patients, utilising computational methods [16, 17]. The angle between the left and right pulmonary arteries (LPA and RPA, respectively) appear to influence valve regurgitation and the post-operative hemodynamics [8, 14, 15]. However, further analysis is required on the geometry-dependent effects on the underlying mechanisms of flow within the pulmonary bifurcation.

This study presents a preliminary computational investigation of the flow development

in idealised two-dimensional models of the pulmonary bifurcation, using physiological vessel dimensions and boundary conditions. Five different geometries were created with varying angles between the main pulmonary artery (MPA) and its branches (Section 2). Computational fluid dynamic results are presented, including velocity streamlines, velocity and pressure distribution, and wall shear stress profiles (Section 3). These results contribute to a better understanding of the hemodynamic environment in the pulmonary bifurcation and may help identify a flow-dependent metric that could determine the optimal timing for pulmonary valve replacement.

2 MATERIALS AND METHODS

2.1 Pulmonary arterial geometries

Five different geometries, which represent the pulmonary bifurcation, were created in SolidWorks^{TM}. A schematic representation of the models is presented in Figure 1. In all models, the diameter of the main pulmonary artery (MPA), D, is assumed 26 mm [18], while the diameters of the left and right pulmonary arteries (LPA, RPA, respectively) are assumed equal, both at 20 mm ($0.77D$). These values are physiologically relevant, observed in healthy subjects [18]. To investigate the effect of the angle between the main pulmonary artery and its branches, on the flow, the following geometries were assumed:

(a) a symmetric Y-Junction with the angle between MPA and both branches being 120^o (similar, on average, to pulmonary bifurcations of normal subjects [14], Figure 1a),

(b) an asymmetric Y-Junction where the MPA–LPA angle is 100^o and the MPA–RPA angle is 150^o (previously related to pulmonary bifurcations of CHD patients [15]). Figure 1b presents three variations for this junction, with the following specifications, to investigate further geometric effects:
   (i) Model 1 assumes a common origin (at O) for the MPA and branch centrelines (Figure 1b-i);
   (ii) Model 2 has a common origin for the MPA and LPA, at point O, while the RPA centreline originates at $0.1154D$ upstream of O (Figure 1b-ii);
   (iii) Model 3 assumes displaced origins for both the LPA and RPA centrelines, by $0.1154D$ downstream and $0.3846D$ upstream of point O (Figure 1b-iii),

(c) a T-Junction where the angle between the MPA and both branches is 90^o, representing the extreme case of LPA kinking [15, 8] (Figure 1c).

In all models, the MPA length (measured as the distance from the MPA inlet to point O) is set to $3.85D$ and the length of each of the LPA and RPA branches (measured from the MPA centreline to the branch outlet) is $2.3D$. A fillet of radius $0.38D$ was used to join the top and side walls of the junction, in all models. Figure 1a displays additionally the location of a reference line (RL), indicated by arrows in the symmetric Y-Junction, and the topWall, as both are used in the analysis.

2.2 Mesh generation requirements

The computational mesh was generated using the commercial software ANSA v17.1, BETA CAE Systems. An initial investigation was conducted to assess the influence

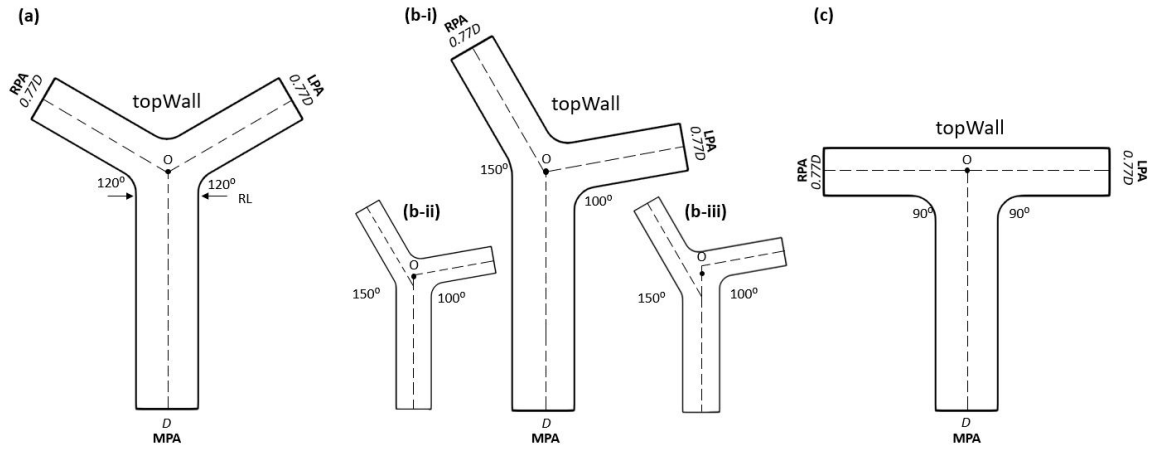

Figure 1: A schematic representation of five different models assumed for the pulmonary bifurcation, where D is the diameter of the main pulmonary artery (MPA): (a) a symmetric Y-Junction; (b) an asymmetric Y-Junction in three variations, (b-i) model 1, (b-ii) model 2, (b-iii) model 3 (downsized by 0.6 times); and (c) a T-Junction. The arrows in (a) indicate a reference line (RL) used later in the analysis, and the topWall boundary. LPA: Left pulmonary artery. RPA: Right pulmonary artery.

of different element types on the computational solution, for the particular geometries. Although triangular elements are usually preferred for more complex models of the pulmonary arteries, they may induce non-orthogonality issues in OpenFOAM®. To that end, two meshes were tested for the symmetric Y-Junction model, with roughly the same total number of elements: (a) 4798 (Figure 2a) and (b) 4888 (Figure 2b) total number of elements, which included primarily quadrilateral and triangular elements, respectively; in both cases, a boundary layer of quadrilateral elements was adopted close to the walls of the artery, in order to capture the near-wall velocities and shear stresses in the bifurcation. The effect of element type was evaluated by calculating the integral of the velocity profile along the x-position at the reference line (Figure 1a). No difference was found between the individual integrals. The quadrilateral elements were adopted in this study to facilitate simulations with the selected solver. The decision regarding the elements used have been previoulsy validated by Arbia et al. (2014), where better results were obtained when axisymmetric elements oriented along the direction of flow were used [19].

A grid independence analysis was also performed in the symmetric Y-Junction model (Figure 2c), using quadrilateral-based meshes with various total numbers of elements (Table 1). The velocities of the models were compared taking into account the maximum velocity magnitude at the reference line. In the presented results, meshes with a total number of approximately 5000 elements were used for all models, as grid independency results were obtained for a total number of elements above 4798.

Table 1: Grip independence analysis for the symmetric Y-Junction model (Figure 2a).

Test	1	2	3	4	5	6
Total number of elements	148	367	1246	3090	4798	6638

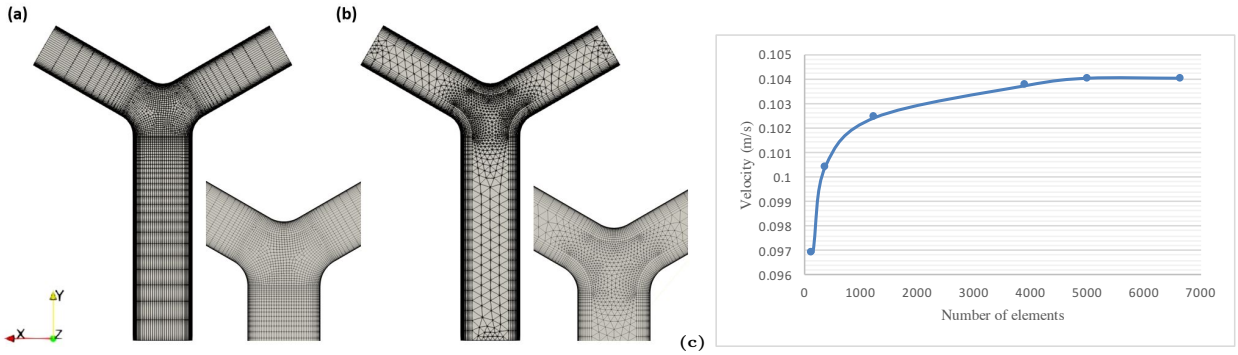

Figure 2: Computational grids of the pulmonary models with a surface mesh of (a) primarily quadrilateral elements and (b) primarily triangle elements. A boundary layer mesh is adopted near the walls of the models. (c) Grip independence analysis test, based on the maximum velocity value obtained at the reference point of the symmetric Y-Junction model.

2.3 Numerical approximations

The computational simulations were performed assuming steady, fully-developed laminar flow at the MPA inlet. Blood was considered incompressible, governed by the Newtonian Navier-Stokes equations:

$$\nabla \cdot \vec{u} = 0 \tag{1}$$

$$\rho \frac{\partial u}{\partial t} + \rho(u \cdot \nabla)u = -\nabla \mathrm{p} + \mu \nabla^2 u \tag{2}$$

where $u = [u_x, u_y, u_z]$ is the velocity vector, ρ is the fluid density, p is the static pressure and μ is the dynamic viscosity. The density and viscosity of the blood were ρ =1060 kg/m^3 and $\mu = 4 \cdot 10^{-3}$ Pa s, respectively [8].

Flow is characterised by the Reynolds number:

$$Re = UD/\nu \tag{3}$$

where U is a characteristic velocity, here the mean MPA velocity, and ν the kinematic viscosity of the fluid. In all models presented here, a parabolic velocity profile was assigned at the inlet boundary of the MPA, with a mean velocity U of 0.1 m/s, which corresponds to a Reynolds number of 650. The velocity was chosen by taking into account averaged mean velocities observed in pulmonary arteries of healthy subjects [20, 21]. A zero-pressure condition was assigned at the RPA and LPA boundaries, expressed relative to the normal mean pulmonary artery pressure at rest (8-20 mm Hg). The numerical calculations were performed using the simpleFoam solver of OpenFOAM®, for steady incompressible, laminar flow. The walls of the models were assumed rigid and no-slip boundary condition were assigned.

2.4 Computational analysis

To characterise the flow development in the arterial models of Figure 1, streamlines and contours of velocity, pressure distribution, and wall shear stress profiles were extracted. Velocity values were non-dimensionalised by dividing all values with the mean inlet value.

Wall shear stress values were non-dimensionalised by the value at the inlet walls. Possible boundary effects were investigated and the boundary conditions were found not to impact the results for the assumed Reynolds number.

3 RESULTS

In this study, the effect of the angle on the heamodynamics of the pulmonary bifurcation was investigated using five different geometries (Figure 1), at Reynolds number 650. Figure 3 presents streamlines of (a) the symmetric Y-Junction (Figure 3a), (b) the asymmetric Y-Junction, in three model variations (Figure 3b-i, 3b-ii, 3b-iii,), and (c) the T-Junction (Figure 3c). Arrows along the streamlines indicate the direction of fluid flow from the main pulmonary artery (MPA) to the daughter branches, the left (LPA) and right (RPA) pulmonary arteries. Recirculation zones are observed near the walls for the 90^o, 100^o and 120^o branching angles, in regions downstream of the reference line (RL), which is at the entrance to the junction. An extended recirculation area was seen for the 100^o branching angle of the LPA, at the asymmetric Y-Junction model 1 (Figure 3b-i), while no recirculation zone was found for the 150^o branching angle of the RPA, in the same model. The asymmetric Y-Junction models 2 and 3 (Figure 3b-ii, 3b-iii) exhibited, however, small recirculation zones at the origin of the RPA.

Figures 4 and 5 display contours of non-dimensional velocity and pressure distribution, respectively, for (a) the symmetric Y-Junction (Figure 4a), (b) the asymmetric Y-Junction, in three model variations (Figure 4b-i, 4b-ii, 4b-iii,), and (c) the T-Junction (Figure 4c) respectively; the non-dimensionalisation is based on division with the mean velocity assigned at the inlet (MPA). Red colour indicates higher value of velocity, while blue colour represents lower values. Higher velocities are observed along the centre of the MPA for all models, with lower velocities occurring adjacent to the walls. The stagnation point (indicated with an arrow and the letter S in Figure 4) was identified for all models, at the point of zero local velocity, with clear higher pressure values (Figure 5). The stagnation point for the symmetric Y-Junction, the T-Junction, and model 3 of the asymmetric Y-Junction was found along the MPA centreline, whereas for models 1 and 2 of the asymmetric Y-Junction the stagnation point was 0.003235 D and 0.001646 D, respectively, towards the LPA.

Wall Shear Stress (WSS) profiles along the topWall (as noted in Figure 1) are plotted in Figure 6, non-dimensionalised by the value at the inlet walls (equal to 0.3364 $kg/m \cdot s^2$, or 3.364 $dynes/cm^2$). The x-axis in the plots has been normalised, based on D, and the plots were moved so that the stagnation point falls at zero position for all models, to represent distance from the stagnation point. The results indicate a significant increase of the WSS in the RPA for model 1 of the asymmetric Y-Junction, as compared to the symmetric Y-Junction and the T-Junction (Figure 6a), and even higher WSS values for models 2 and 3 (Figure 6b). In the LPA, model 1 of the asymmetric Y-Junction shows similar WSS values to the symmetric Y-Junction, both of which exhibit higher WSS than the T-Junction. However, WSS values in the LPA of model 3 are smaller than those in model 1, and close to values of the T-Junction; model 2 shows intermediate values of WSS.

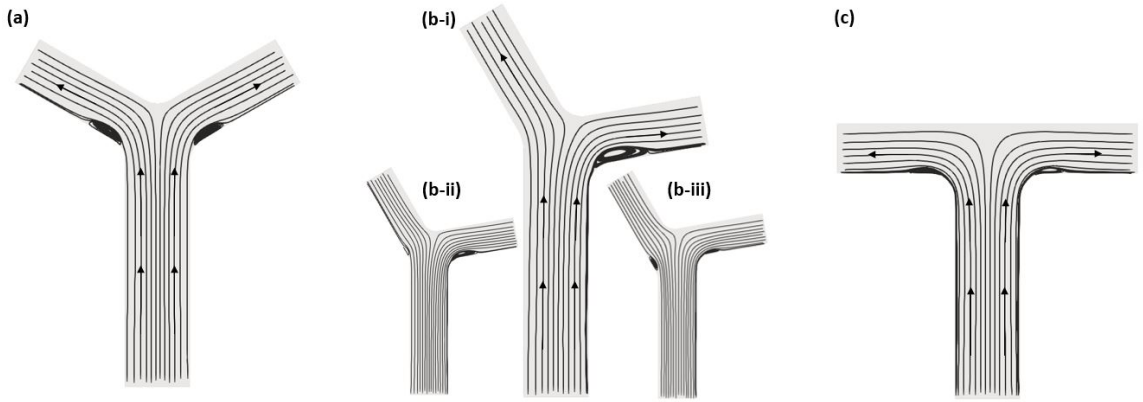

Figure 3: Velocity streamlines in (a) the symmetric Y-Junction; (b) the asymmetric Y-Junction in three variations, (b-i) model 1, (b-ii) model 2, (b-iii) model 3; and (c) the T-Junction, for a Reynolds number of 650. Recirculation zones are visible downstream of the bifurcation entrance at a 90^o, 100^o and 120^o angle. Arrows indicate the direction of fluid flow.

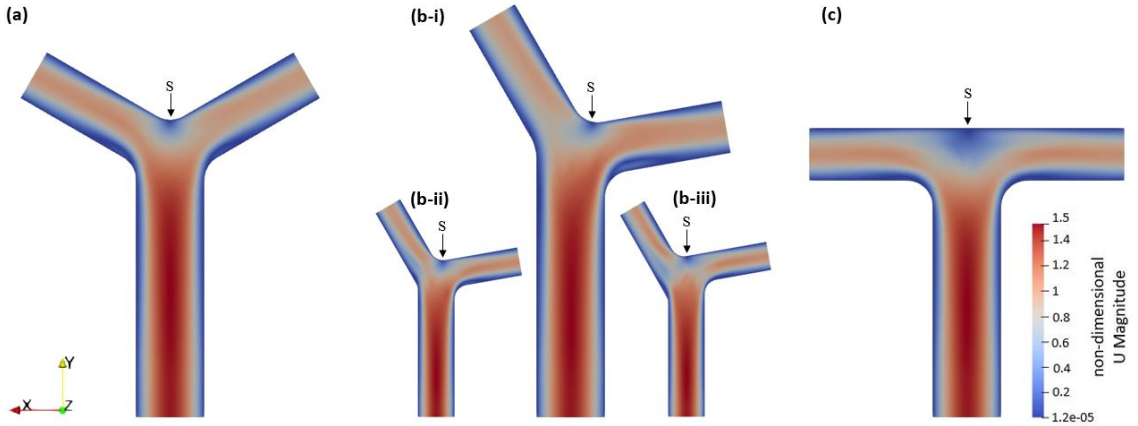

Figure 4: Contours of non-dimensional velocity, based on the mean inlet velocity, in (a) the symmetric Y-Junction; (b) the asymmetric Y-Junction in three variations, (b-i) model 1, (b-ii) model 2, (b-iii) model 3; and (c) the T-Junction (Re=650). The stagnation point (S) is indicated in all models.

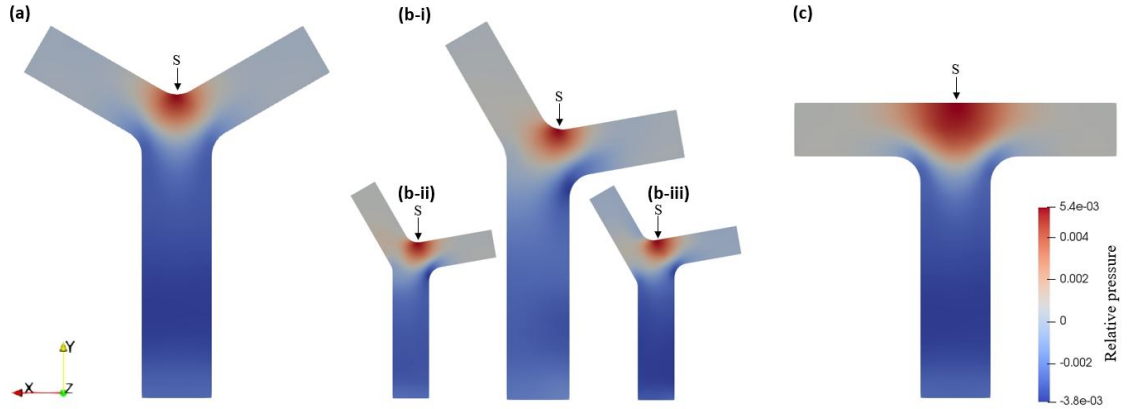

Figure 5: Pressure distribution in (a) the symmetric Y-Junction, (b) the asymmetric Y-Junction, and (c) the T-Junction (Re=650). Pressure values are expressed relative to the normal mean pulmonary artery pressure at rest (8-20 mm Hg). The stagnation point (S) is indicated in all models.

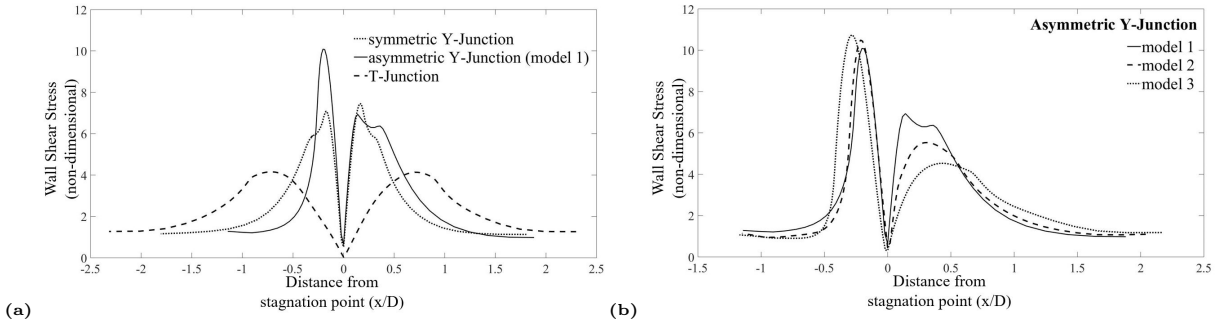

Figure 6: Wall shear stress profiles along the the topWall. The x-axis in the plots has been normalised, based on D, and the plots were moved so that the stagnation point falls at zero position for all models, to represent distance from the stagnation point.

4 DISCUSSION

Congenital heart defects constitute a great challenge to the medical sector, with an increasing number of studies focusing on the anticipated clinical outcomes and possible treatments. Repaired tetralogy of Fallot patients often require re-operations, primarily due to valve regurgitation, generated over the years after repair of the right ventricular outflow trunk and pulmonary branch re-stenosis or kinking. Pulmonary valve replacement is deemed essential for those patients, however the correct timing for re-operation is often unclear and relies on symptoms. Many studies lately focus on characterising the hemodynamic environment in the pulmonary artery using computational methods, either to better understand the effect of various geometric and hemodynamic conditions, or to visualise new surgical procedures [15, 14, 17, 19, 22, 23, 24, 25, 26, 27, 28].

In this study, we presented a preliminary investigation on the effect of the angle of the pulmonary bifurcation through different computational models. A symmetric Y-Junction was assumed first, with the angles between the main pulmonary artery and its branches being 120^o. This geometry represents control adults, as the angles of healthy left and right pulmonary branches have been found approximately at 112^o and 125^o angle with the MPA, respectively [14]. Subsequently, an asymmetric Y-Junction was considered, with a 100^o angle of LPA with MPA and a 150^o angle of RPA with MPA, which is more representative of patients with ToF [14]. This junction was modelled in three variations to investigate the effect of the origin of branches. Finally, a fifth case was created, based on a T-Junction (90^o angle between MPA and both LPA, RPA), which could be seen as an extreme case of LPA kinking [14, 8]. Streamlines, velocity and pressure distribution, and wall shear stress profiles were compared to assess the effects of angle and geometrical features on the flow development within the pulmonary bifurcation.

Streamlines in all models (Figure 3) demonstrated the existence of recirculation zones in the majority of the branching angles (90^o, 100^o, and 120^o angles), for both the LPA and RPA, immediately downstream of the entrance to the junction; however, an increase of the branching angle (Figures 3a, 3b-i, and 3c) does not appear to correlate with increasing regions of recirculation zones, for the same Reynolds number, as the recirculation zone for the 100^o angle (Figure 3b-i) is more extended than for 90^o and 120^o. Model variations for the 150^o angle had a less clear impact on the velocity streamlines, as model 1 showed no

recirculation zone in the RPA, wheres models 2 and 3 had some recirculation occurring at the entrance, for the same bifurcation angle and Reynolds number. Previous studies that investigated the effect of angle in the pulmonary bifurcation using angles between 90^o and 150^o, have found development of recirculation zones for bifurcation angles at and below 100^o [14, 8]. Zhang et al. (2016) [8] investigated the effect of the LPA branching angle on flow within the RPA, for a much higher Reynolds number of 7000, and observed that recirculation zones developed at the lower wall of the entrance to the RPA, when the angle of the LPA declined to 120^o. On the other hand, Chern et al. (2012), did not observe any recirculation zones in normal subject with 112^o angle of LPA and 125^o of RPA [14]. The results of the current study are in agreement with Chern et al. (2008) [15] where recirculation was observed in the 100^o angle, but not in the 150^o angle (if model 1 is assumed for the asymmetric Y-Junction), and with Tang et al. (2012) [18] were swirling flows were observed in the proximal arteries of normal subjects. However, our results for models 2 and 3 of the asymmetric Y-Junction differ with the above studies, demonstrating that the development of a recirculation zone in the RPA is affected by the origin of the branch, for the same branching angle.

The velocity distribution was compared in the different models and no abrupt changes were observed, except for model 3 of the asymmetric Y-Junction, where smaller local velocity values were seen around the junction. As expected, higher velocities were observed at the centre of the main pulmonary artery of the models, with the lower velocities near the walls due to the no-slip boundary condition. Moderate velocities were identified in the centre of the branches of the pulmonary models. A rapid drop is also apparent at the entrance to the pulmonary branches, with the local velocity becoming zero instantaneously, at the stagnation point. These results are in agreement with velocity patterns found in various previous studies [26, 27, 29] and with identified effects of bifurcation angle [8]. As the flow from the main pulmonary artery, impinges upon the wall between LPA and RPA, the stagnation point becomes an area of highest relative pressure. High values were also found in a region around the stagnation point for all models, the extent of which varied for each model; it was enlarged for the T-Junction and moderate for all junctions, with slight eccentric areas for models 2 and 3 of the asymmetric Y-Junction.

Wall shear stress is one of the most important hemodynamic parameters, particularly for its role in the function of endothelial cells in the systemic circulation and the development of atherosclerosis [30]. In this study, WSS profiles were plotted for all models along the top wall, expressed as normalised distance from the stagnation point, to allow comparison.

WSS along the top wall of the bifurcation increases with increasing branching angle, for both LPA and RPA; however WSS is also dependent on the origin of each branch (as demonstrated in Figure 6b), having a greater effect on the LPA. To the best of the author's knowledge, the latter has not been studied before.

Several limitations exist in this study, including primarily the assumptions of two-dimensional geometries, and non-pulsatile flow, however the results offer an important evaluation of some key geometrical effects on the flow in models of the pulmonary bifurcation. The novelty of this work is two-fold: it makes a direct comparison of various

simplified models of the pulmonary bifurcation, by changing the branching angle, and demonstrates a new effect of the branching origin on the hemodynamic conditions. Further investigation is required for the asymmetric Y-Junction.

Future work will involve further investigation of the effect of geometric and hemodynamic parameters, including higher Reynolds numbers. Stenosed pulmonary branches will be created and the effect of Reynolds number will be tested. In addition, 3-D patient-specific computational models, pre- and post-operative of the pulmonary valve replacement will be reconstructed using MRI image data of adult patients with repaired tetralogy of Fallot. The hemodynamic characterisation of these models will be crucial for the identification of a computational metric to assess the right timing for the pulmonary valve replacement, which remains ambiguous. Such a metric can be particularly valuable for both the clinicians and the patients, as it could help towards a more timely decision-making and better surgical outcomes.

ACKNOWLEDGEMENTS

This work is supported in part from the University of Strathclyde Research Studentship Scheme (SRSS) Research Excellence Awards (REA), Project No 1208, and the European Union's Horizon 2020 research and innovation programme under the Marie Skłodowska-Curie grant agreement No 749185.

REFERENCES

[1] Mitchell S.C., Korones S.B., Berendes H.W. Congenital Heart Disease in 56,109 Births Incidence and Natural History. *Circulation* (1971) **43**:323-332.

[2] MacMahon B., McKeown T., Record R.G. The Incidence and Life Expectation of Children with Congenital Heart Disease. *Heart* (1953) **15**:121-129.

[3] Cetta F., Lictenberg R.C., Clark S.E. Adults with congenital heart disease. *Comprehensive therapy* (1992) **18**:33-37.

[4] Perloff J.K. Congenital Heart Disease in Adults. A new Cardiovascular Subspecialty. *Circulation* (1991) **84**:1881-1890.

[5] Rao B.N.S., Anderson R.C., Edwards J.E. Anatomic variations in the tetralogy of Fallot. *American Heart Journal* (1971) **81**:361-371.

[6] Brickner M.E., Hillis L.D., Lange R.A. Congenital Heart Disease in Adults. Second of two parts. *New England Journal of Medicine* (2000) **342**:334-342.

[7] Gatzoulis M.A., Webb G.D., Daubeney P.E.F. *Diagnosis and Management of Adult Congenital Heart Disease*. Elsevier (2017) 474-488.

[8] Zhang W., Liu J., Yan Q., Liu J., Hong H., Mao L. Computational haemodynamic analysis of left pulmonary artery angulation effects on pulmonary blood flow. *Interactive CardioVascular and Thoracic Surgery* (2016) **23**:519-525.

[9] Harris M.A., Whitehead K.K., Gillespie M.J., Liu T.Y., Cosulich M.T., Shin D.C., Goldmuntz E., Weinberg P.M., Fogel M.A. Differential Branch Pulmonary Artery Regurgitant Fraction is a Function of Differential Pulmonary Arterial Anatomy and Pulmonary Vascular Resistance. *Cardiovascular Imaging* (2011) **4**:506-513.

[10] Warner K.G., O?Brien P., Rhodes J., Kaur A., Robinson D.A., Payne D.D. Expanding the Indications for Pulmonary Valve Replacement After Repair of Tetralogy of Fallot. *The Society of Thoracic Surgeons* (2003) **76**:1066-1072.

[11] Buechel E.R.V., Dave H.H., Kellenberger C.J., Dodge-Khatami A, Pretre R., Berger F., Bauersfeld U. Remodelling of the right ventricle after early pulmonary valve replacement in children with repaired tetralogy of Fallot: assessment by cardiovascular magnetic resonance. *European Heart Journal* (2005) **26**:2721-2727.

[12] Lee C., Kim Y.M., Lee C.H., Kwak J.G., Park C.S., Song J.Y., Shim W.S., Choi E.Y., Lee S.Y., Baek J.S. Outcomes of Pulmonary Valve Replacement in 170 Patients with Chronic Pulmonary Regurgitation After Relief of Right Ventricular Outflow Tract Obstruction. *Journal of the American College of Cardiology* (2012) **60**:1005-1014.

[13] Randles A., Frakes D.H., Leopold J.A. Computational Fluid Dynamics and Additive Manufacturing to Diagnose and Treat Cardiovascular Disease. *Trends in Biotechnology* (2017) **35**:1049-1061.

[14] Chern M.J., Wu M.T., Wei-Her S. Numerical Study for Blood Flow in Pulmonary Arteries after Repair of Tetralogy of Fallot. *Computational and Mathematical Methods in Medicine* (2012) **2012**:1-18.

[15] Chern M.J., Wu M.T., Wang H.L. Numerical investigation of regurgitation phenomena in pulmonary arteries of Tetralogy of Fallot patients after repair. *Journal of Biomechanics* (2008) **41**:3002-3009.

[16] Guibert R., McLeod K., Caiazzo A., Mansi T., Fernandez M.A., Sermesant M., Pennec X., Vignon-Clementel I., Boudjemline Y., Gerbeau J.F. Group-wise construction of reduced models for understanding and characterization of pulmonary blood flows from medical images. *Medical Image Analysis* (2014) **18**:63-82.

[17] Kilner P.J., Balossino R., Dubini G., Babu-Narayan S.V., Taylor A.M., Pennati G., Migliavacca F. Pulmonary regurgitation: the effects of varying pulmonary artery compliance, and of increased resistance proximal or distal to the compliance. *International Journal of Cardiology* (2009) **133**:157-166.

[18] Tang B.T., Pickard S.S., Chan R.P., Tsao P.S., Taylor C.A., Feinstein J.A. Wall Shear stress is decreased in the pulmonary arteries of patients with pulmonary arterial hypertension: An image-based, computational fluid dynamics study. *Pulmonary Circulation* (2012) **2**:470-476.

[19] Arbia G., Corsini C., Moghadam M.E., Marsden A.L., Migliavacca F., Pennati G., Hsia T.Y., Vignon-Clementel E.I. Numerical blood flow simulation in surgical corrections: what do we need for an accurate analysis?. *Journal of Surgical Research* (2014) **186**:44-55.

[20] Gabe I.T., Gault J.H., Ross J., Mason D.T., Mills C.J., Schillingford J.P., Braunwald E. Measurement of Instantaneous Blood Flow Velocity and Pressure in Conscious Man with a Catheter-Tip Velocity Probe. *Circulation* (1969) **40**:603-614.

[21] Bronzino J. *The Biomedical Engineering Handbook*, Second Edition. CRC Press LLC (2000) 30-3.

[22] Spilker R.L., Feinstein J.A., Parker D.W., Reddy V.M., Taylor C.A. Morphometry-Based Impedance Boundary Conditions for Patient-Specific Modeling of Blood Flow in Pulmonary Arteries. *Annals of Biomedical Engineering* (2007) **35**:546-559.

[23] Das A., Banerjee R.K., Gottliebson W.M. Right Ventricular Inefficiency in Repaired Tetralogy of Fallot: Proof of Concept for Energy Calculations form Cardiac MRI Data. *Annals of Biomedical Engineering* (2010) **38**:3674-3687.

[24] Guibert R., McLeod K., Caiazzo A., Mansi T., Fern?ndez M.A., Sermesant M., Pennec X., Vignon-Clementel I.E., Boudjemline Y., Gerbeau J.F. Group-wise construction of reduced models for understanding and characterization of pulmonary blood flows from medical images. *Medical Image Analysis* (2014) **18**:63-82.

[25] Kheyfets V.O., Rios L., Smith T., Schroeder T., Mueller J., Murali S., Lasorda D., Zikos A., Spotti J., Reilly J.J., Final E.A. Patient-specific computational modeling of blood flow in the pulmonary arterial circulation. *Computer Methods and Programs in Biomedicine* (2015) **120**:88-101.

[26] Berdajs D.A., Moshabi S., Charbonnier D., Hullin R., von Segesser L.K. Analysis of flow dynamics in right ventricular outflow tract. *Journal of Surgical Research* (2015) **197**:50-57.

[27] Berdajs D., Moshabi S., Vos J., Charbonier D., Hullin R., von Segesse L.K. Fluid dynamics simulation of right ventricular outflow tract oversizing. *Interactive Cardio-Vascular and Thoracic Surgery* (2015) **21**:176-182.

[28] Tang D., Yang C., Geva T., Rathod R., Yamauchi H., Gooty V., Tang A., Kural M.H., Billiar K.L., Gaudette G., del Nido P.J. A Multiphysics Modeling Approach to Develop Right Ventricle Pulmonary Valve Replacement Surgical Procedures with a Contracting Band to Improve Ventricle Ejection Fraction. *Comput Struct* (2013) **122**:78-87.

[29] Moshabi S., Mickaily-Huber E., Charbonnier D., Hullin R., Burki M., Ferrari E., von Segesser L., Berdajs D.A. Computational fluid dynamics of the right ventricular outflow tract and of the pulmonary artery: a bench model of flow dynamics. *Interactive CardioVascular and Thoracic Surgery* (2014) **19**:611-616.

[30] Chiu J.J., Usami S., Chien S. Vascular endothelial responses to altered shear shress: Pathologic implications for atherosclerosis. *Annals of Medicine* (2009) **41**: 19-28.